

Changing the type of superconductivity by magnetic and potential scattering

V. G. Kogan^{1,*} and R. Prozorov^{1,†}

¹Ames Laboratory - DOE and Department of Physics, Iowa State University, Ames, IA 50011

(Dated: 16 October 2014)

By evaluating the upper and thermodynamic critical fields, H_{c2} and H_c , and their ratio H_{c2}/H_c at arbitrary temperatures, we argue that situations are possible when a type-II material is transformed to type-I by adding magnetic impurities.

I. INTRODUCTION

Traditionally, classification of isotropic superconductors as type-I and II is based on the value of the Ginzburg-Landau parameter $\kappa = \lambda/\xi$, the ratio of the London penetration depth and the coherence length. At the critical temperature T_c , $\kappa = 1/\sqrt{2}$ separates type-II materials for which $\kappa > 1/\sqrt{2}$ from the type-I where $\kappa < 1/\sqrt{2}$. At T_c , the upper and thermodynamic critical fields are related by $H_{c2} = \sqrt{2}\kappa H_c$ so that their ratio $R = H_{c2}/H_c = 1$ if $\kappa = 1/\sqrt{2}$. In type-II materials $H_{c2} > H_c$ that is equivalent to $\kappa > 1/\sqrt{2}$, in other words, at T_c the criteria for the type-II $\kappa > 1/\sqrt{2}$ and $R > 1$ are equivalent. However, for $T < T_c$, where the critical fields as well as λ and ξ can be evaluated using the microscopic theory,¹ the relation $H_{c2} = \sqrt{2}\kappa H_c$ no longer holds. For the type-II superconductivity we need of course $H_{c2} > H_c$ or $R > 1$. Hence, the GL κ criterion cannot be used, except at T_c .²

Parameter R was calculated in the clean limit for anisotropic Fermi surfaces and order parameters and possibilities of changes in the type of superconductivity with temperature or the applied field direction were demonstrated.² Still, the question arises of how R depends on scattering? It is well known that non-magnetic impurities cause H_{c2} to increase.³ Effect of magnetic impurities is just the opposite, H_{c2} is suppressed.^{4,5} On the other hand, the thermodynamic critical field H_c (along with the condensation energy) is insensitive to the transport scattering, but is reduced by the pair-breaking.⁵⁻⁷ It is difficult to evaluate scattering effects for arbitrary anisotropies, here we limit ourselves to isotropic s-wave superconductors with arbitrary transport and magnetic scattering (in Born approximation).

Evaluating H_{c2} we use extensively Ref. 4 to which we refer the readers interested in derivation of formulas we employ. For H_c we make use of the review by Maki.⁷ We show that pair-breaking scattering may suppress H_{c2} faster than H_c and even cause transition from the type-II to the type-I superconductivity. By using specific material parameters for Th, we show a way of making this, initially type-I superconductor, to become type-II upon introduction of non-magnetic disorder, and then turn it back to type-I by *adding* magnetic scattering. Our theory contains a single material parameter - the clean-limit κ_{GL} at T_c - so that our results can be readily applied to other isotropic materials.

II. $T \rightarrow T_c$

Here we compare the slopes of $H_{c2}(T)$ and $H_c(T)$ at T_c . We use dimensionless variables

$$t = \frac{T}{T_c}, \quad h = H_{c2} \frac{\hbar^2 v^2}{2\pi T_c^2 \phi_0}, \quad (1)$$

and the scattering parameters

$$\rho = \frac{\hbar}{2\pi T_c \tau}, \quad \rho_m = \frac{\hbar}{2\pi T_c \tau_m}, \quad \rho^\pm = \rho \pm \rho_m, \quad (2)$$

where τ and τ_m are times of the transport and pair-breaking scattering. At T_c one has for isotropic s-wave materials:⁴

$$-\frac{dh}{dt}\Big|_{t=1} = 3\rho_-^2 \left[1 - \rho_m \psi' \left(\rho_m + \frac{1}{2} \right) \right] / \left[\psi \left(\rho_m + \frac{1}{2} \right) - \psi \left(\frac{\rho^+ + 1}{2} \right) + \frac{\rho_-}{2} \psi' \left(\rho_m + \frac{1}{2} \right) \right], \quad (3)$$

where ψ is the digamma function. The actual slope is

$$\frac{dH_{c2}}{dT}\Big|_{T_c} = \frac{2\pi\phi_0 T_c}{\hbar^2 v^2} \frac{dh}{dt}\Big|_{t=1}. \quad (4)$$

According to Ref. 7 (or 6):

$$\frac{dH_c}{dT}\Big|_{T_c} = -2\pi\sqrt{8\pi N(0)} \frac{1 - \rho_m \psi'(\rho_m + 1/2)}{\sqrt{b_1(\rho_m)}}, \quad b_1 = -\frac{1}{2}\psi'' \left(\rho_m + \frac{1}{2} \right) - \frac{\rho_m}{6}\psi''' \left(\rho_m + \frac{1}{2} \right); \quad (5)$$

$N(0)$ is the density of states on the Fermi level per spin. The ratio of our interest is:

$$R(T_c) = \frac{H_{c2}}{H_c}\Big|_{T_c} = \frac{dH_{c2}/dT}{dH_c/dT}\Big|_{T_c} = C \frac{T_c}{T_{c0}} \frac{\rho_-^2 \sqrt{-\frac{1}{2}\psi''(\rho_m + \frac{1}{2}) - \frac{\rho_m}{6}\psi'''(\rho_m + \frac{1}{2})}}{\psi(\rho_m + \frac{1}{2}) - \psi(\frac{\rho^+ + 1}{2}) + \frac{\rho_-}{2}\psi'(\rho_m + \frac{1}{2})}, \quad (6)$$

$$C = \frac{3\phi_0 k_B T_{c0}}{\hbar^2 v^2 \sqrt{8\pi N(0)}}. \quad (7)$$

The constant C is, in fact, close to κ_{GL} for the clean case:

$$\kappa_{GL} = \frac{3\phi_0 T_{c0}}{\hbar^2 v^2 \sqrt{7\zeta(3)\pi N(0)}} = C \sqrt{\frac{8}{7\zeta(3)}} = 0.975 C. \quad (8)$$

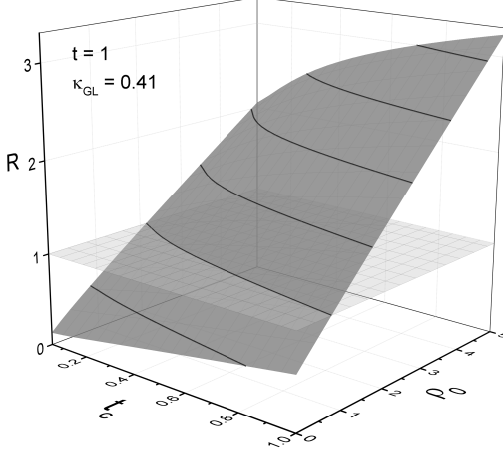


FIG. 1. The ratio of slopes of H_{c2} and H_c at T_c for $\kappa_{GL} = 0.41$. Instead of the second coordinate $0 < \rho_{m0} < 0.14$ we use directly $1 > t_c = T_c/T_{c0} > 0$. The horizontal plane is $R = 1$.

According to Abrikosov-Gor'kov (AG),⁵

$$\frac{T_c}{T_{c0}} = \exp \left[-\psi \left(\rho_m + \frac{1}{2} \right) + \psi \left(\frac{1}{2} \right) \right] \quad (9)$$

One can check that for $\rho_m \rightarrow 0$, $R(T_c) \rightarrow \sqrt{2} \kappa_{GL}$.

The scattering parameters (2) are convenient in analytical work. Being T_c dependent, while T_c depends on ρ_m , they are not good for comparison with data. It is better to work with T_c independent material parameters

$$\rho_{m0} = \frac{\hbar}{2\pi T_{c0} \tau_m} = \rho_m \frac{T_c}{T_{c0}}, \quad \rho_0 = \frac{\hbar}{2\pi T_{c0} \tau} = \rho \frac{T_c}{T_{c0}}. \quad (10)$$

It is better yet to plot the ratio R as a function of ρ_0 and $t_c = T_c/T_{c0}$ instead of ρ_{m0} . The way to do this is described in Appendix A. Results of numerical evaluation of $R(T_c)$ are shown in Fig. 1. We have chosen for $\kappa_{GL} = 0.41$ having in mind possible applications for Th.⁸ The ratio R increases nearly linearly with increasing transport ρ_0 for any t_c . However, for a fixed ρ_0 , R decreases when the pair-breaking intensifies. Of course, for large enough transport scattering (in this case for $\rho_0 > 5$) the material is type-II for any pair-breaking. We show below that for relatively clean samples unusual scenarios are possible.

III. $T = 0$

The dimensional quantity h of Eq.(4) for $t \rightarrow 0$ has been evaluated in Ref. 4 for any ρ and ρ_m . The upper critical field is given by

$$H_{c2} = \frac{2\pi T_{c0}^2 \phi_0}{\hbar^2 v^2} t_c^2 h = H^* t_c^2 h. \quad (11)$$

The constant H^* is close to the clean limit $H_{c2}(0) = \pi T_{c0}^2 \phi_0 e^{2-\gamma} / 2\hbar^2 v^2$ ($\gamma = 0.577$ is the Euler constant);³ in

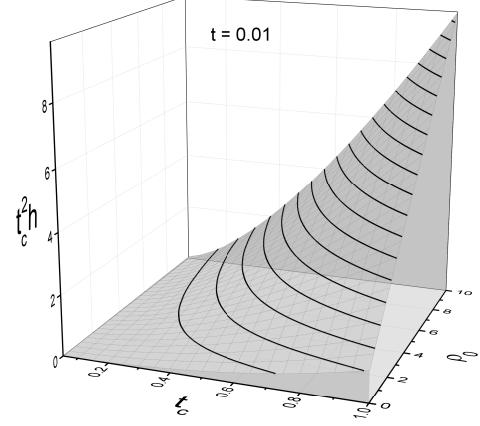


FIG. 2. The quantity $t_c^2 h = H_{c2}(0)/H^*$ is plotted versus ρ_0 and $t_c = T_c/T_{c0}$. To reduce the calculation time $t = 0.01$ is taken instead of $t = 0$,

fact, $H^*/H_{c2}(0) = 4e^{\gamma-2} = 0.964$. The dimensionless $t_c^2 h$ versus ρ_0 and t_c is shown in Fig. 2.

We now calculate $H_c(0) = \sqrt{8\pi F(0)}$, where evaluation of the condensation energy $F(0)$ requires knowledge of the order parameter $\Delta(\rho_m)$. The latter satisfies:⁵

$$\frac{\Delta}{\Delta_0} = e^{-\pi\zeta/4}, \quad \zeta = \frac{\hbar}{\tau_m \Delta} \leq 1, \quad (12)$$

$$\frac{\Delta}{\Delta_0} = e^{\eta(\zeta)}, \quad \zeta > 1, \quad (13)$$

$$\eta = -\cosh^{-1} \zeta - \frac{\zeta}{2} \sin^{-1} \frac{1}{\zeta} + \frac{\sqrt{\zeta^2 - 1}}{2\zeta}, \quad (14)$$

where $\Delta_0 = T_{c0} \pi e^{-\gamma}$ is the zero- T gap of a clean sample. The condensation energy at $T = 0$ is given by:^{6,7}

$$\frac{2F(0)}{N(0)\Delta^2} = 1 - \frac{\pi}{2}\zeta + \frac{2}{3}\zeta^2, \quad \zeta \leq 1, \quad (15)$$

$$\frac{2F(0)}{N(0)\Delta^2} = 1 - \zeta \sin^{-1} \frac{1}{\zeta} + \zeta^2 \left(1 - \sqrt{1 - 1/\zeta^2} \right) - \frac{\zeta^2}{3} \left(1 - (1 - 1/\zeta^2)^{3/2} \right), \quad \zeta > 1. \quad (16)$$

It is convenient to normalize F on the clean limit value

$$F_0(0) = \frac{N(0)\Delta_0^2}{2} = \frac{N(0)T_{c0}^2 \pi^2}{2e^{2\gamma}}. \quad (17)$$

Then, Eq. (15) for $\zeta \leq 1$ transforms to:

$$f = \frac{F}{F_0} = e^{-\pi\zeta/2} \left(1 - \frac{\pi}{2}\zeta + \frac{2}{3}\zeta^2 \right), \quad (18)$$

where Eq. (12) has been used. Clearly, $f = 1$ for $\zeta = 0$.

For $\zeta > 1$, we have:

$$f = \frac{F}{F_0} = e^{2\eta} \left[1 - \zeta \sin^{-1} \frac{1}{\zeta} + \zeta^2 \left(1 - \sqrt{1 - 1/\zeta^2} \right) - \frac{\zeta^2}{3} \left(1 - (1 - 1/\zeta^2)^{3/2} \right) \right]. \quad (19)$$

We obtain:

$$H_c = \sqrt{8\pi F_0 f} = \Delta_0 \sqrt{4\pi N(0) f(\rho_m)} = H_{c0} \sqrt{f(\rho_m)}, \quad (20)$$

where H_{c0} is the thermodynamic critical field at $T = 0$ in the absence of magnetic impurities.

Now $R(0) = H_{c2}/H_c$ at $T = 0$ can be evaluated:

$$R(0) = \frac{\phi_0 T_{c0} e^\gamma}{\hbar^2 v^2 \sqrt{\pi N(0)}} \frac{t_c^2 h}{\sqrt{f}} = D \frac{t_c^2 h}{\sqrt{f}}, \quad (21)$$

where the dimensionless constant is given by

$$D = \frac{\phi_0 T_{c0} e^\gamma}{\hbar^2 v^2 \sqrt{\pi N(0)}} = \frac{e^\gamma \sqrt{7\zeta(3)}}{3} \kappa_{GL} \approx 1.72 \kappa_{GL}. \quad (22)$$

The ratio $R(0)$ evaluated numerically is shown in Fig. III for $\kappa_{GL} = 0.41$.

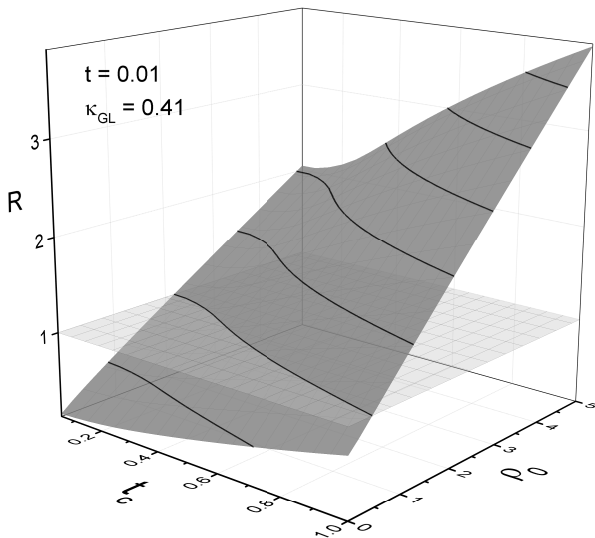


FIG. 3. The ratio $R(0) = H_{c2}/H_c$ at $T = 0$ for $\kappa_{GL} = 0.41$. The plane $R = 1$, the boundary between two types of superconductivity, is also shown.

Figure 4 shows curves along which $R(\rho_0, t_c) = \text{const}$ at $T = T_c$ and $T = 0$. The contour $R(\rho_0, t_c) = 1$ separates the upper part of the plane (t_c, ρ_0) where $R > 1$ and which corresponds to the type-II and the lower part where $R < 1$, the type-I. We note that the curves of constant $R(T_c)$ and $R(T = 0)$ meet in the limit of strong pair-breaking; this can be shown analytically, but we omit a cumbersome proof. This result could be expected: when $t_c \rightarrow 0$, the temperature domain between 0 and T_c shrinks to zero as well and, therefore, we must have $R(0) = R(T_c)$.

Also, we observe that these curves cross at a certain level of pair-breaking, e.g., at $t_c^* \approx 0.5$ for $R = 1$. Clearly, the point t_c^* separates narrow domains between solid and dashed lines on the phase plane (t_c, ρ_0) with different behavior of the material in question with changing temperature. Within the narrow part where $t_c > t_c^*$, the

material is type-I near T_c and becomes type-II at some temperature on cooling toward 0. Within the narrow region where $t_c < t_c^*$, it is of the type-I near 0 and becomes type-II at some temperature on warming toward T_c .

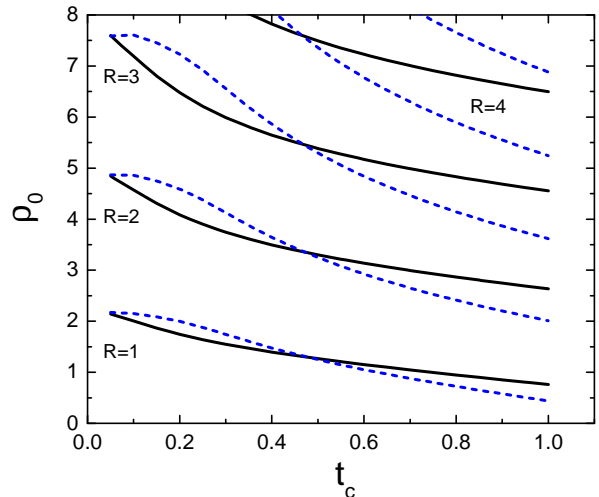


FIG. 4. (Color online) Solid lines: contours of $R(t_c, \rho_0) = \text{const}$ for $T = T_c$. Dashed lines are for $T = 0$. Both sets are calculated for $\kappa_{GL} = 0.41$.

IV. DISCUSSION

In many new-discovered materials, superconductivity coexists or competes with antiferromagnetism. Fe-based materials are an example. Pair-breaking scattering is likely to be present and affect superconducting properties in various ways. Our work for isotropic s-wave case does not pretend to adequately describe these properties, given that the only material parameter entering our theory is κ_{GL} . Although oversimplified, the isotropic example may provide a qualitative guidance to such questions as the type of superconductivity, needed for understanding the material behavior in magnetic fields.

Besides, these questions have a fundamental relevance since historically the classification of superconductors to two types came from the GL theory which holds only near the critical temperature. It is long known that most of pure elemental metals are of the type-I and can be turned type-II by addition of non-magnetic scatterers. We show here that the magnetic scattering may reduce H_{c2} faster than H_c thus pushing materials toward type-I.

One of such scenarios is illustrated in Fig. 5 for a material with $\kappa_{GL} = 0.41$ (the value reported for the clean Th). Let the originally type-I clean material (point a) be doped with non-magnetic impurities to become type-II (point b). If now pair-breaking impurities are added, t_c is reduced and the material may reach the region under contours $R(0; t_c, \rho_0) = 1$ and $R(T_c; t_c, \rho_0) = 1$ which corresponds to type-I at all T s. We note that the type-I

superconductivity emerging due to magnetic impurities is likely to be gapless, since it may appear at small t_c .

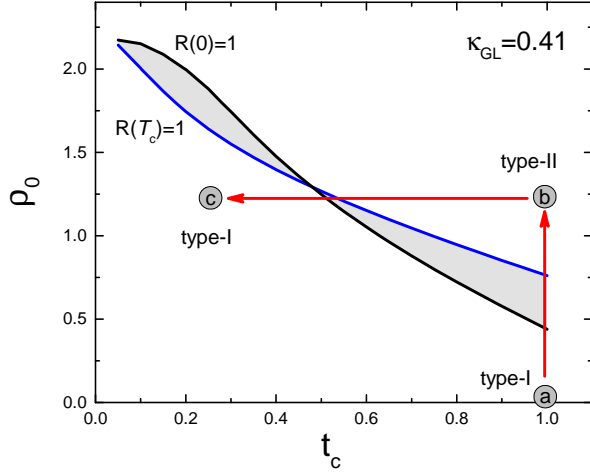


FIG. 5. (Color online) Contours of $R(t_c, \rho_0) = 1$ for $T = T_c$ and $T = 0$ for $\kappa_{GL} = 0.41$.

Interesting questions about possible change of the superconductivity type with changing temperature (for material parameters in shaded areas of Fig. 5), possible fluctuations near this transition, peculiarities of intervortex interactions ect, are out of the scope of this article, and may be addressed if a material with proper characteristics is found.

The authors are grateful to D. Finnemore, J. Kirtley, J. Thompson, P. Canfield, S. Bud'ko, V. Taufor, and B. Maple for many helpful discussions. The Ames Laboratory is supported by the Department of Energy, Office of Basic Energy Sciences, Division of Materials Sciences and Engineering under Contract No. DE-AC02-07CH11358.

Appendix A: Numerical procedure

The scattering parameters ρ and ρ_m of Eq. (2) are not convenient variables for comparison with experimental data; they depend on T_c which itself is determined by the Eq. (9) containing $\rho_m(T_c)$. Instead one can use material parameters ρ_0 (roughly, the ratio of the BCS coherence length and the mean free path) and ρ_{m0} proportional to the pair-breaking scattering rate. Furthermore, ρ_{m0} is uniquely related by Eq. (9) to the actually measured T_c , so that ρ_0 and T_c are the two independent parameters we use to present our results.

Within our numerical scheme, this amounts to: (1) for a given t_c , solving Eq. (9) for ρ_m ; then (2) forming ρ_m and ρ according to Eq. (10) in terms of ρ_{m0} and ρ_0 , and (3), having ρ_m and ρ , evaluating the slopes of H_{c2} and H_c at T_c , or calculating numerically $H_{c2}(0)$ and $H_c(0)$ with the help of the procedure developed in Ref. 2 where Mathlab has been used.

Appendix B: Strong pair-breaking

Given a quite involved numerical procedure for evaluation of the ratios $R(t_c, \rho_0)$, it is useful to have analytic results at least at some limiting points. We consider here the strong pair-breaking limit $t_c \rightarrow 0$. In this case, $h(0)$, related to $H_{c2}(0)$, has been derived in Ref. 2:

$$h(0) = \frac{1}{8} \left(\frac{\rho^-}{\rho_m} \right)^2 \left(\frac{\rho^-}{2\rho_m} + \ln \frac{2\rho_m}{\rho^+} \right)^{-1}. \quad (B1)$$

Since all $\rho \propto 1/T_c$, their ratios and $h(0)$ are T_c independent. In particular,

$$\frac{\rho}{\rho_m} = \frac{\rho_0}{\rho_{m0}} = 4e^\gamma \rho_0 \quad (B2)$$

where we replaced ρ_{m0} with its critical value $\rho_{m0,cr} = e^{-\gamma}/4$. Hence, in this limit $h(0)$ depends only on ρ_0 .

The critical fields at $T = 0$ are

$$H_{c2} = \frac{2\pi T_c^2 \phi_0}{\hbar^2 v^2} h(0), \quad H_c = \frac{\Delta^2 \tau_m \sqrt{\pi N(0)}}{\hbar \sqrt{3}}, \quad (B3)$$

where $H_c(0)$ is obtained by going to $\zeta \rightarrow \infty$ in the free energy (16). Taking into account that at $T = 0$ for the strong pair-breaking $\Delta^2 = 2\pi^2 T_c^2$ ^{5,7} we obtain:

$$R(0)|_{t_c \rightarrow 0} = \frac{\sqrt{3} \phi_0}{\pi \hbar v^2 \sqrt{\pi N(0)}} \frac{h(0; \rho_0, \rho_{m0,cr})}{\tau_m} \Big|_{t_c \rightarrow 0}. \quad (B4)$$

Here, $\tau_m \rightarrow 2\hbar/\Delta_0$, the critical value at which $t_c = 0$. This can also be written in terms of κ_{GL} of Eq. (8):

$$R(0)|_{t_c \rightarrow 0} = \frac{7\zeta(3)e^{-\gamma}}{2\sqrt{3}} \kappa_{GL} h(0; \rho_0, \rho_{m0,cr}). \quad (B5)$$

By setting here $R(0) = 1$ and solving numerically this equation for a given κ_{GL} , we can find the value of ρ_0 at which the curve $R(0; t_c, \rho_0) = 1$ reaches $t_c = 0$. This gives $\rho_0 = 2.21$ for $\kappa_{GL} = 0.41$ in agreement with what is shown in Fig. 5. Similarly, we can verify all other limiting points of both $R(0; t_c, \rho_0) = 1$ and $R(T_c; t_c, \rho_0) = 1$ to confirm our numerical results.

* kogan@ameslab.gov

† prozorov@ameslab.gov

¹ G. Eilenberger, Phys. Rev. **153**, 584 (1967).

² V. G. Kogan and R. Prozorov, Phys. Rev. B, **90**, 054516

(2014).

³ E. Helfand, N.R. Werthamer, Phys. Rev. **147**, 288 (1966).

⁴ V. G. Kogan and R. Prozorov, Phys. Rev. B, **88**, 024503 (2013).

- ⁵ A.A. Abrikosov and L.P. Gor'kov, Zh. Eksp. Teor, Fiz. **39**, 1781 (1060) [Sov. Phys. JETP, **12**, 1243 (1961)].
- ⁶ Skalsky et al, Phys. Rev. **136**, A1500 (1964).
- ⁷ K. Maki in *Superconductivity* ed. by R. D. Parks, Marcel Dekker, New York, 1969, v.2, p.1035.
- ⁸ W. R. Decker and D. K. Finnemore, Phys. Rev. **172**, 430 (1968).